

*Journal of*  
***Mechanics of***  
***Materials and Structures***

**DETERMINATION OF MODE I STRESS INTENSITY FACTORS OF  
COMPLEX CONFIGURATIONS USING STRAIN GAGES**

S. Swamy, M. V. Srikanth, K. S. R. K. Murthy and P. S. Robi

***Volume 3, N° 7***

***September 2008***



mathematical sciences publishers



## **DETERMINATION OF MODE I STRESS INTENSITY FACTORS OF COMPLEX CONFIGURATIONS USING STRAIN GAGES**

S. SWAMY, M. V. SRIKANTH, K. S. R. K. MURTHY AND P. S. ROBI

Among techniques for the determination of the mode I stress intensity factors (SIFs), strain gage procedures are the simplest and most straightforward. We report here on an experimental investigation of the determination of opening mode stress intensity factors using the single strain gage method. Our approach overcomes certain drawbacks and greatly widens the applicability of strain gage methods in the determination of static SIFs of complex configurations. The approach was tested through experiments on specimens of finite width and finite height edge-cracked plates (fully finite plates) subjected to tensile stress. We compared the experimentally determined mode I stress intensity factors of fully finite plates with the computed values using finite element analysis, obtaining good agreement between the present approach and computed values.

### **1. Introduction**

Cracks frequently initiate and grow at stress concentration zones such as notches, holes, reentrant corners and welded joints in structural components. Because such elements occur frequently in structural components, understanding the severity of cracks is important in the development of static strength, fatigue crack growth and fatigue life prediction methodologies. The stress intensity factor (SIF) is the key parameter in linear elastic fracture mechanics (LEFM) for quantifying the severity of cracks. It reflects the effect of loading, crack size, crack shape and component geometry in life and strength prediction methods.

An accurate knowledge of the stress intensity factor is essential for the prevention of brittle fractures arising from cracks; in particular, the use of the LEFM principles in preventing the fracture of engineering components depends largely on the availability of accurate SIFs. As a result, analytical, numerical and experimental methods for SIF determination in cracked bodies have been developed for several decades [Sanford 2003]. Analytical methods are limited to simple configurations due to mathematical difficulties, and one must resort to numerical or experimental methods for more complex situations. The experimental determination of stress intensity factors is also needed as a way to validate theoretical and numerical results, and provides a valuable aid to their application. Approaches include the compliance method [Bonesteel et al. 1978; Jr 1981], photoelasticity [Gdoutos and Theocaris 1978; Hyde and Warrior 1990], caustics [Theocaris 1970; Konsta-Gdoutos 1996] and strain gage methods [Dally and Berger 1993].

Of all these techniques, the most straightforward is the use of electrical resistance strain gages [Sanford 2003]. It has received much attention because it can measure surface strains accurately and directly within strain gradient zones, allowing the subsequent determination of SIFs. Irwin [1957] first suggested the use of strain gages to determine SIFs; however, the local yielding effect at the crack tip of metallic materials, high strain gradients, the three-dimensional state of stress at the crack tips and the finite size of the strain

*Keywords:* stress intensity factor, strain gage, finite width, PMMA, edge crack, finite height.

gages are the primary issues for establishing a valid approach for accurate measurement of SIFs using the strain gage techniques. Earlier attempts to measure SIFs using strain gages were reported in [Broek 1982].

A practical method to tackle the issues mentioned in the previous paragraph, providing an effective strain gage technique for measuring the static opening mode stress intensity factor ( $K_I$ ) in two-dimensional bodies, was first proposed by Dally and Sanford [1987] for linear elastic isotropic materials. In this method the strains are represented by three/four parameter series. The generalized Westergaard approach [Sanford 1979] is employed to determine the strain series and subsequently  $K_I$ . The chief advantage of the Dally–Sanford approach is that only a single strain gage is sufficient to determine the mode I SIF, which can be placed at distances far away from the crack tip. Their numerical results reveal that the zone of three-parameter strain series is sufficiently large. Further, an analysis of the error due to strain gradient effects was presented, to suggest possible locations for the finite-sized strain gages. Experiments were conducted on aluminum compact tension (CT) specimens with small strain gages (active grid size  $0.76 \times 0.76 \text{ mm}^2$ ) at different distant radial locations from the crack tip. The authors noticed that the gage readings at all locations were affected by the formation of a plastic zone and the subsequent redistribution of stresses and strains. A methodology has been suggested based on Irwin's method of shifting the elastic field [Sanford 2003] by a distance equal to the plastic zone radius  $r_p$  to correct the measured strains, and hence the SIFs. However, a major limitation of this approach is that one should know the exact SIF of the selected configuration a priori in order to calculate the plastic zone size.

Parnas and Bilir [1996] employed the Dally–Sanford single strain gage method to determine the SIFs of CT specimens made of steel and aluminum. Their investigation included the effect of plate thickness. The accuracy of the measured SIFs was observed to depend on the thickness of the specimen. The results clearly show that in the case of thin plates the linearity between applied load and measured strain is not achieved at all loads: beyond a certain load the relationship is found to be nonlinear. However, the linear relation is observed for thick plates. Parnas and Bilir attributed these effects to the formation of plastic zones in the specimens.

Other strain gage methods designed specifically for measuring static mode I SIFs have been proposed by Wei and Zhao [1997] and Kuang and Chen [1995]. Unlike Dally and Sanford, Wei and Zhao used two strain gages, and adopted Williams' [1957] eigenfunction expansion to determine the truncated strain series. These authors tested their theory on three-point bend steel (TPBS) specimens using  $0.5 \times 0.5 \text{ mm}^2$  active-grid strain gages and reported inaccuracies in the measured SIFs due to the formation of plastic zones. However, the locations of the strain gages were suggested empirically and require knowing a priori knowledge about the plastic zone size, which depends on the unknown exact stress intensity factor of the configuration.

Kuang and Chen [1995], in contrast, approached the problem using near-field strain equations and asymptotic strain expressions. They suggested that strain gages can be placed at distances greater than half the thickness of the specimen from the crack tip despite the fact that at distances larger from the crack tip, the measured strains cannot be accurately represented by asymptotic terms alone. They conducted experiments on steel CT specimens using strip gages containing 10 strain sensors each of  $0.5 \times 0.5 \text{ mm}^2$  active grid size. Contrary to theoretical predictions, the normalized mode I SIF was found to be a function of the applied loads and the thickness of the specimen. The measured SIF was also found to

depend on the angular position relative to the crack axis. However these authors demonstrated that highly inaccurate SIF results are obtained if the strain gages are placed at distances below half the thickness of the specimen. Their measurements at locations away from the crack tip are also affected by plasticity effects. Corrections to the measured strains were suggested, in a manner similar to that of [Dally and Sanford 1987], but contrary to earlier works, no improvement of the measured SIFs was accomplished, even after incorporating plastic zone corrections.

Of these various strain gage methods for measuring opening mode static SIFs, the procedure of Dally and Sanford enjoys the greatest practicability and a solid mathematical background. By contrast, very large numbers of strain gages are needed to measure opening mode SIFs in the overdetermined method proposed by Berger and Dally [1988]. Dally and Sanford's technique has been extended to mixed mode cases [Dally and Berger 1986], which requires four strain gages for determination of the SIFs. A proportional extrapolation technique for determining mixed mode SIFs using strain gages has also been proposed [Itoh et al. 1988]. However, a special strain gage pattern is needed in this technique.

An advantage of strain gage techniques is that they can be employed directly on metallic engineering components to determine the SIF of their configurations. Also important is that numerical and analytical solutions of static SIFs of complex domains can be corroborated via strain gage procedures to provide reliability of the results/methods. For example, many researchers have reported on the application of photoelastic methods [Marloff et al. 1971; Chan and Chow 1979; Amir et al. 1989; Nurse et al. 1994] and caustics [Biak et al. 1995; Lee and Hong 1993] to the determination of static SIFs or the corroboration of analytical and numerical solutions for important configurations. Such application investigations using existing procedures are useful in establishing the experimental methods and make them into a viable alternative in real design situations of great complexity.

In spite of these important applications of strain gage methods, no work has been reported to date on the application of the Dally–Sanford single strain gage procedure to the validation of accurate mode I static SIFs of the complex configurations, so as to establish the usefulness of this technique in real design situations. This is true also of the other strain gage methods.

A critical review of earlier work [Dally and Sanford 1987; Parnas and Bilir 1996; Wei and Zhao 1997; Kuang and Chen 1995] in this field discloses the various drawbacks that prevented further utilization of these methods in the determination of SIFs for important complex configurations: (a) the normalized SIF is found to be function of thickness of the specimen and the applied loads which is obstinate to the theory; (b) the measured strains are severely affected by plastic zone formation and subsequent strain redistribution; (c) while certain approximate procedures have been proposed to correct the measured strains (and hence SIFs), these procedures depend on the unknown exact stress intensity factor of the configuration; (d) there are indications that at times no significant improvements can be achieved even after plastic zone corrections are applied. The last three works referenced at the start of this paragraph employed theoretical values of SIFs for CT and TPBS specimens to correct measured SIFs for plasticity effects. Clearly such corrections are not possible in the case of configurations for which no SIF solutions are available.

These difficulties arise mainly from the use of the metallic specimens in strain gage procedures, although the SIF is independent of the material. The preparation of complex configurations, particularly of cracked specimens, is relatively difficult with metallic materials; great care has to be exercised in creating

sharp natural cracks with intricate orientations. Thus methods such as Dally and Sanford's, which have a sound mathematical basis, may be more effectively exploited by using materials other than metals.

The fact that the SIF is independent of the material is exploited in photoelastic and other experimental methods [Gdoutos 1990; Dally and Riley 1991]. As is well known, polymethylmethacrylate (PMMA), known commercially as Perspex or Plexiglas, is a homogeneous, isotropic and brittle material at room temperatures [Maccagno and Knott 1989]. This material has long been used in studies of many aspects of linear elastic fracture mechanics [Maccagno and Knott 1989; Mukherjee and Burns 1972; Katsamanis and Delides 1988; Xu et al. 2004]. One advantage it offers is that it is relatively easy to introduce sharp natural cracks by pressing a razor blade into the bottom of a notch. PMMA is also inexpensive and easy to fabricate in complex cracked configurations, making it an excellent model material for experimental fracture mechanics. (See [Maccagno and Knott 1989] for details and a historical account of the use of PMMA for this purpose.)

In view of the shortcomings arising to the use of metallic specimens in strain gage procedures and of the availability of excellent strain gage technology, we suggest that the use of the specimens made of PMMA material will greatly broaden the applications of these methods. All of aforesaid drawbacks of use of the metallic specimens can be overcome with the use of this material. However, to the best of our knowledge no published report is available on use of the PMMA in conjunction with strain gage methods, in particular with the single gage technique of Dally and Sanford.

The proximity of component boundaries to the crack tip has an effect on SIFs [Sanford 2003; Gdoutos 1990]. In general, as the boundaries come close to the crack tip, the magnitude of the SIF increases. An edge-cracked plate subjected to uniform tensile stress is a widely used benchmark problem [Pang 1993]. Analytical and numerical solutions for the mode I SIF of this configuration are available only for finite width plates [Murakami 1987; Tada et al. 2000], that is, for large values of  $a/w$  and  $h/w \geq 1$ , where  $a$  is the crack length,  $w$  is the width of the plate and  $h$  is the height of the plate from the crack axis. However, to our knowledge no report in the open literature, whether using analytical, experimental or numerical methods, is available on SIFs for edge-cracked plates of finite width and finite height (large  $a/w$  and  $h/w \leq 1$ ) subjected to uniform tension. In this situation both the width and the height of the plate are close to the crack tip. We call such plates *fully finite*.

In this work we investigate the feasibility of experimental determination of accurate opening mode stress intensity factors using the Dally–Sanford method and cracked polymethylmethacrylate (PMMA) specimens. In the Dally–Sanford procedure, gages can be placed at low strain gradient zones; as a consequence larger gages can be employed. In contrast with [Dally and Sanford 1987; Wei and Zhao 1997; Kuang and Chen 1995], our work attempts to measure accurate SIFs using relatively large strain gages (active gage length 3 mm) and monotonically increasing loads with continuous measurement of the strain. Our goal is to accurately determine opening mode SIFs of fully finite edge-cracked plates subject to uniform tension. To validate the proposed method for the determination of SIFs, we compare our experimental results with computer-calculated values obtained using ANSYS finite-element software.

## 2. Theoretical background

In the Dally and Sanford method [1987], the strain field adjacent to a crack tip is represented by an infinite series solution. The area around a crack tip can be divided into three regions (Figure 1) to identify valid

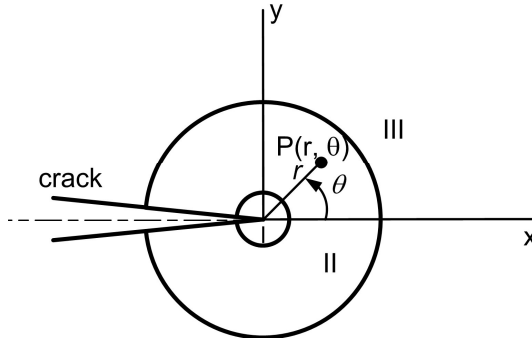


Figure 1. Different regions at the crack tip.

locations for accurate strain measurements. The very near field region (region I in Figure 1) is the zone where the singular term in the series or asymptotic expression is sufficient to represent this region. This is a singularity dominated zone. Due to yielding of material and three-dimensional nature of stress state, this is not a valid region for accurate strain measurements.

Region II is the near-field region, defined as the area beyond region I where the strain field can be represented within a specified accuracy by a small number of series terms, both singular and nonsingular. Region III, the far-field region, corresponds to large values of the radial distance  $r$  from the crack tip; in that region a very large number of unknowns are needed in the series for an accurate representation of the strain field, so strain measurements are not appropriate there. Thus region II is the optimum zone for accurate strain measurements: it can be represented by few terms and is sufficiently away from the crack tip. Dally and Sanford [1987] adopted a three-parameter approach; that is, they assumed that the strain field in region II can be represented with sufficient accuracy by three series terms. The strain field in this region for plane stress conditions is then written as (see also [Sanford 2003])

$$\begin{aligned}
 E\varepsilon_{xx} &= A_0r^{-1/2} \cos \frac{\theta}{2} \left( (1-\nu) - (1+\nu) \sin \frac{\theta}{2} \sin \frac{3\theta}{2} \right) + 2B_0 + A_1r^{1/2} \cos \frac{\theta}{2} \left( (1-\nu) - (1+\nu) \sin^2 \frac{\theta}{2} \right), \\
 E\varepsilon_{yy} &= A_0r^{-1/2} \cos \frac{\theta}{2} \left( (1-\nu) - (1+\nu) \sin \frac{\theta}{2} \sin \frac{3\theta}{2} \right) - 2\nu B_0 + A_1r^{1/2} \cos \frac{\theta}{2} \left( (1-\nu) - (1+\nu) \sin^2 \frac{\theta}{2} \right), \\
 2G\gamma_{xy} &= A_0r^{-1/2} \left( \sin \theta \cos \frac{3\theta}{2} \right) - A_1r^{1/2} \left( \sin \theta \cos \frac{\theta}{2} \right),
 \end{aligned}$$

where  $A_0$ ,  $A_1$  and  $B_0$  are unknown coefficients that can be determined using the geometry of the specimen and the boundary conditions. Using the definition of  $K_I$  one can easily show that it is related to  $A_0$  by

$$K_I = \sqrt{2\pi} A_0. \tag{2}$$

A single strain gage is sufficient to measure the constant  $A_0$  (hence  $K_I$ ) by placing and orienting the strain gage as given below. Using the strain transformation equations, the strain component  $\varepsilon_{x'x'}$  at the point  $P$  located by  $r$  and  $\theta$  (Figure 2) is given by

$$\begin{aligned}
 2G\varepsilon_{x'x'} &= A_0r^{-1/2} \left( k \cos \frac{\theta}{2} - \frac{1}{2} \sin \theta \sin \frac{3\theta}{2} \cos 2\alpha + \frac{1}{2} \sin \theta \cos \frac{3\theta}{2} \sin 2\alpha \right) \\
 &\quad + B_0(k + \cos 2\alpha) + A_1r^{1/2} \cos \frac{\theta}{2} \left( k + \sin^2 \frac{\theta}{2} \cos 2\alpha - \frac{1}{2} \sin \theta \sin 2\alpha \right), \tag{3}
 \end{aligned}$$

where  $\kappa = \frac{1-\nu}{1+\nu}$ .

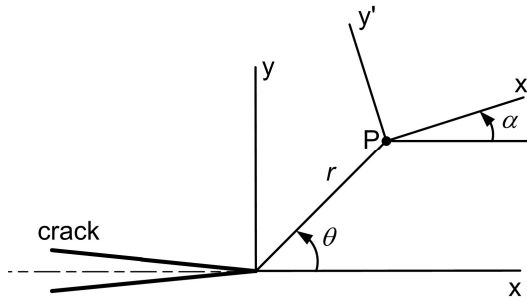


**Figure 2.** Strain gage location and orientation.

The coefficient  $B_0$  term in (3) can be eliminated by selecting the angle  $\alpha$  so that

$$\cos 2\alpha = -\kappa = -\frac{1-\nu}{1+\nu}. \tag{4}$$

The coefficient  $A_1$  can also be made zero if the angle  $\theta$  is selected so that

$$\tan \frac{\theta}{2} = -\cot 2\alpha. \tag{5}$$

Thus by placing a single strain gage (Figure 2) with  $\alpha$  and  $\theta$  as defined by (4) and (5) one can measure the strain  $\varepsilon_{x'x'}$ , which in turn is related to  $K_I$  by

$$2G\varepsilon_{x'x'} = \frac{K_I}{\sqrt{2\pi r}} \left( k \cos \frac{\theta}{2} - \frac{1}{2} \sin \theta \sin \frac{3\theta}{2} \cos 2\alpha + \frac{1}{2} \sin \theta \cos \frac{3\theta}{2} \sin 2\alpha \right). \tag{6}$$

The angles  $\alpha$  and  $\theta$  depend only on the Poisson’s ratio of the specimen material. The selection of the radius  $r$  for locating the strain gage can be obtained by considering strain gradient effects, as explained in [Dally and Sanford 1987]. Since the gages can be located far from high strain gradient zones, the measurements can be taken with relatively large, hence inexpensive, strain gages.

### 3. Numerical evaluation of the SIFs of fully finite edge-cracked plates

The SIFs of finite width and finite height edge-cracked plates is given by

$$K_I = \sigma \sqrt{\pi a} F_I \left( \frac{a}{w}, \frac{h}{w} \right), \tag{7}$$

where  $F_I \left( \frac{a}{w}, \frac{h}{w} \right)$  is the configuration factor or normalized SIF, which shows the effect of geometry of the body on the SIF [Sanford 2003; Gdoutos 1990].

Finite element analyses using ANSYS 9.0 were carried out to determine accurate opening mode SIFs of fully finite edge-cracked plates (with various values of  $a/w$  and  $h/w$ ) subject to uniform tension (Figure 3). The displacement extrapolation method of ANSYS [2005] was employed to compute the normalized opening mode SIFs. It is known (see [Swain 2007]) that this method is consistent and yields very accurate SIFs. In our investigation we chose two values of  $a/w$ , 0.3 and 0.5, and values of  $h/w$  ranging from 0.2 to 1.1 in steps of 0.1. It is well known that semi-infinite plates can be represented approximately by  $h/w \geq 1$ , while  $h/w < 1$  represents fully finite edge-cracked configurations.



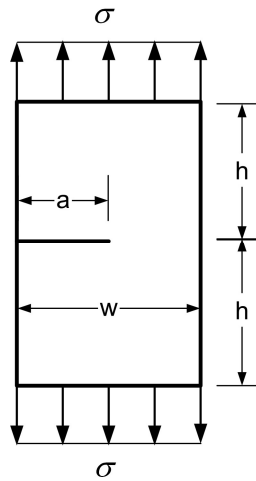


**Figure 3.** Problem domain: Edge cracked plate subjected to uniform tension.

Natural isoparametric quadratic triangular elements (T6) and the corresponding quarter point singular elements [Barsoum 1976; Freese and Tracey 1976] were used. We assume plane stress conditions,  $\sigma = 1.0$  MPa, a Young’s modulus  $E = 10000$  MPa and a Poisson’s ratio of 0.3. Because of symmetry, only half the plate was considered in the analysis. Figure 4 shows a typical unstructured mesh pattern (without gradation) used in the determination of the normalized SIFs. Such meshes were used for all values of  $a/w$  and  $h/w$ . No significant improvements in the SIFs were observed when the meshes were refined further [Swamy 2007].

The computed normalized opening mode SIFs for different values of  $a/w$  and  $h/w$  are presented in Table 1. As expected, the SIF increases as the  $a/w$  ratio increases and the  $h/w$  ratio decreases, that is,

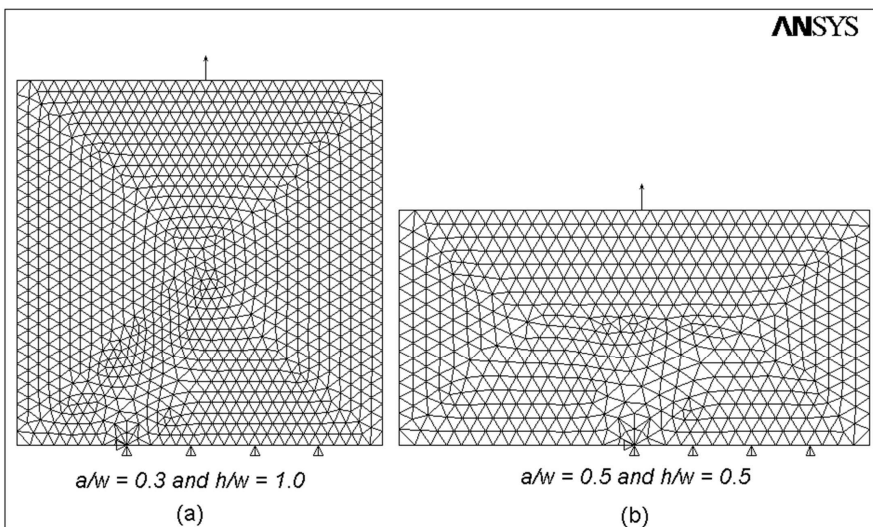


**Figure 4.** Typical meshes for SIF determination for the problem domain.

$h/w$	$F_I = K_I/\sigma\sqrt{\pi a}$		$h/w$	$F_I = K_I/\sigma\sqrt{\pi a}$	
	$a/w = 0.3$	$a/w = 0.5$		$a/w = 0.3$	$a/w = 0.5$
0.2	3.5979	6.0343	0.7	1.6938	2.8514
0.3	2.5390	4.0308	0.8	1.6733	2.8342
0.4	2.0736	3.2898	0.9	1.6649	2.8277
0.5	1.8496	3.0060	1.0	1.6622	2.8250
0.6	1.7420	2.8954	1.1	1.6613	2.8249

**Table 1.** FE-computed normalized SIFs of semi-infinite and finite edge-cracked plates.

when the surrounding boundaries approach the crack tip. It may also be noticed from Table 1 that  $F_I$  remains almost constant for  $h/w \geq 0.9$ , indicating semi-infinite cases.

### 4. Experimental details

As stated, our goal was to determine the SIFs of fully finite edge-cracked panels with the shape shown in Figure 3, using the single strain gage technique of [Dally and Sanford 1987]. The configuration of the experimental specimens representing the problem domain is shown in Figure 5. The specimens were made from commercially available PMMA (Perspex sheet) with a thickness of 6 mm. Plane stress condition is anticipated in the specimens. The width of all the specimens was kept at  $w = 150$  mm, while the crack length  $a$  and the height  $h$  of the specimen were varied to create semi-infinite and fully finite edge-cracked specimens.

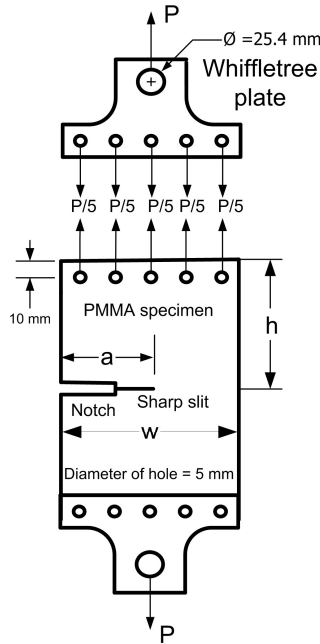


**Figure 5.** Details of the experimental PMMA specimen.

All specimens were monotonically loaded with a closed loop, servohydraulic INSTRON 8801 machine (100 kN capacity) under displacement control with actuator speed 0.05 mm/min. The whiffletree technique (Figure 5) was employed to transform the point load from the INSTRON to a uniformly distributed load on the specimen. The whiffletree plates were made from mild steel, and mild steel pins were used to connect them with the specimens. Five holes were used to connect each whiffletree to the corresponding specimen. As shown in Figure 5, each hole lies 10 mm from the top or bottom edge of the specimen. It was assumed that the point load applied by the machine is equally divided between the five holes as shown in Figure 5.

To imitate the sharp crack form the model (Figure 3), we made a 3 mm wide notch with a jigsaw, of length  $(a-2)$  mm, and further created a fine slit, 2 mm long, by means of a razor blade. Very sharp cracks can be made in this way: the crack tip root radius is less than 0.0035 mm (see [Srikanth 2006]). Two  $a/w$  ratios (0.3 and 0.5) and four  $h/w$  ratios (0.3, 0.5, 0.7 and 1.0) were chosen for the experimental study. Only one specimen each was tested for  $a/w = 0.3$  and various values of  $h/w$ , and two specimens each for  $a/w = 0.5$  and various  $h/w$ . Strain measurements on the loaded specimens were carried out using a single electrical strain gage (HBM type 1-LY11-3/120) with an active grid of  $3 \times 1.4 \text{ mm}^2$ . A Young's modulus of 2300 MPa and Poisson's ratio of 0.37 have been measured for the PMMA material in a tensile test [Swamy 2007]. Thus  $\alpha$  and  $\theta$  in (4) and (5) equal respectively  $58.69^\circ$  and  $54.76^\circ$ . The radial position of the strain gage  $r = 10$  mm was chosen in all experiments based on the strain gradient analysis presented in [Dally and Sanford 1987].

The measured strains were processed and digitized using a National Instruments Data Acquisition Board (PXI 1052) and an eight-channel universal strain gage module (SCXI 1520). Continuous strain measurements was made by interfacing the INSTRON machine's load cell with a NI Data Acquisition Board (DAQ). Figure 6 depicts a specimen attached to the INSTRON with whiffletree plates.

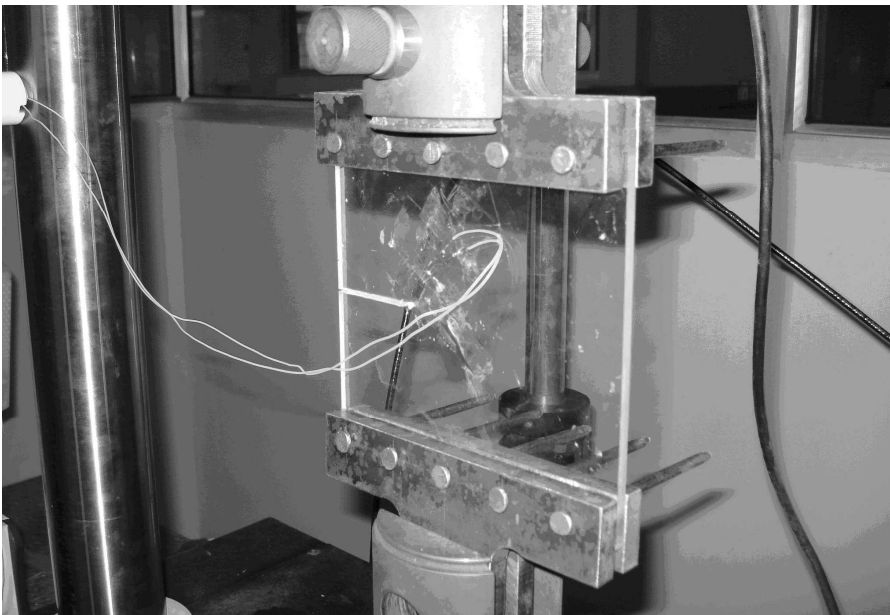


**Figure 6.** A typical PMMA specimen with whiffletree plates.

**5. Finite element simulation of the experimental specimens**

Since the experimental specimen (Figure 5) differs from the original problem domain (Figure 3) especially in the matter of loading, a finite element simulation of the experimental specimen with assumed magnitude of point loads at the five holes was carried out using ANSYS. Such simulations before the experiments are vital in establishing whether or not the selected configuration of the experimental specimen mimics the actual problem domain. The specimens were modeled with T6 elements and quarter-point singular elements were placed at the crack tips. Figure 7 shows a representative mesh with loading and boundary conditions employed in the numerical simulation studies.

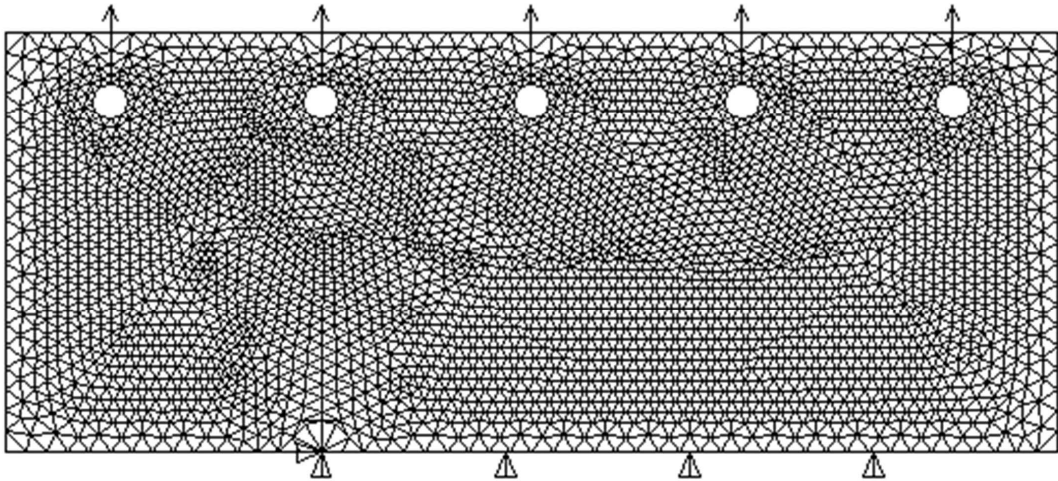


**Figure 7.** Typical mesh of an experimental specimen, computed by ANSYS.

A few results of computed SIFs of the experimental specimens and that of original problem domain are presented in Table 2. It also presents the percent relative error (in absolute value) considering SIFs in Table 1 as exact values. It may be noticed from table that, the expected SIFs from the specimens are in very good agreement with the SIFs of the original problem (Figure 3). Although not presented here, similar simulations were carried out for other values of  $h/w$  and exceptional agreement between the two set of SIFs was observed [Swamy 2007]. Thus the numerical results clearly indicate that experimental specimen as designed in Figure 5 can accurately imitate the original problem (Figure 3).

	$h/w$	0.4	0.6	1.0
specimen $F_I$ (Figure 5)		2.0652	1.7427	1.6655
problem domain $F_I$ (Figure 3)		2.0736	1.7420	1.6622
relative error		0.41%	0.04%	0.20%

**Table 2.** Experimental and computed normalized SIFs for  $a/w = 0.3$  and selected values of  $h/w$ .

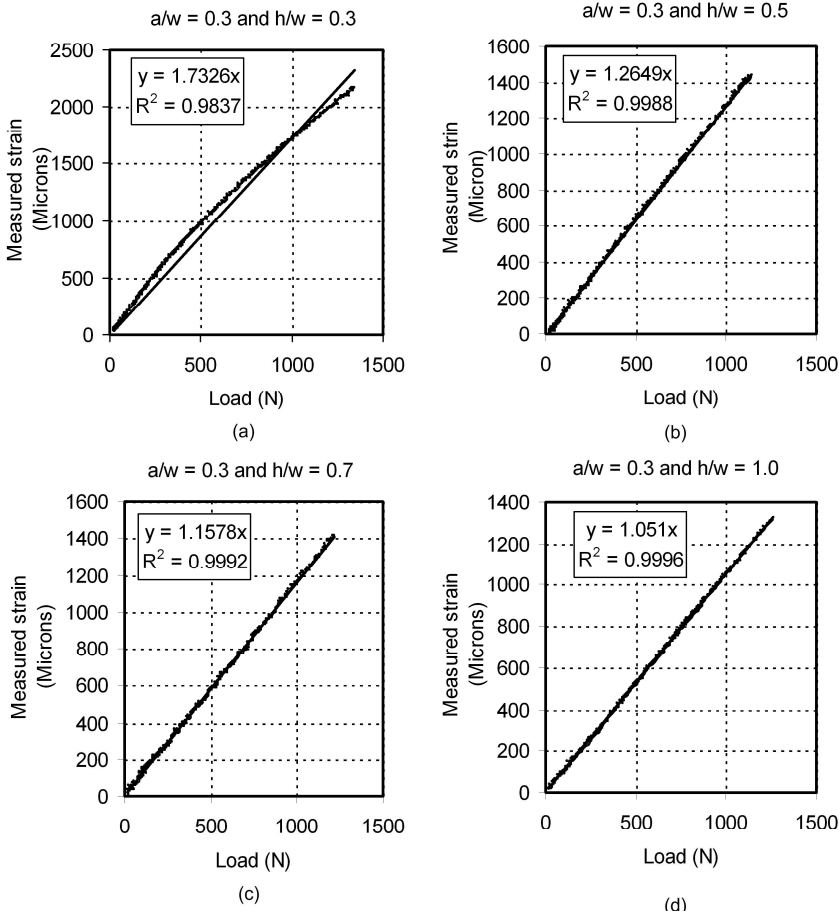


**Figure 8.** Variation of the measured strain with applied load for  $a/w = 0.3$ .

### 6. Experimental results and discussion

Figure 8 shows the experimentally measured strain data on PMMA specimens as a function of the applied load for  $a/w = 0.3$  and  $h/w = 0.3, 0.5, 0.7, 1.0$ . A linear fit was made to the data points of all the specimens. A very good linear relationship can be noticed between the measured strain and the applied load in the figure for all four specimens. The coefficient of determination  $R^2$  in all the graphs is also close to unity, indicating good fits. A slight deviation from linearity in Figure 8(a) is probably due to the improper settlement of the pins in the holes of the whiffletree. From the linear equations presented in each of the four graphs, measured strains were calculated at different loads. Subsequently, using the computed strains the opening mode SIFs were determined using (6) at different values of applied load.

Table 3 presents the measured opening mode SIFs ( $K_I$ ) at different loads for semi-infinite and fully finite edge-cracked plates of  $a/w = 0.3$ . The experimental results of Table 3 are presented in graphical form in Figure 9 to show the dependency of  $K_I$  on the applied load and proximity to the boundaries. Since the measured strains are linearly proportional to the applied load so are the measured SIFs. Besides

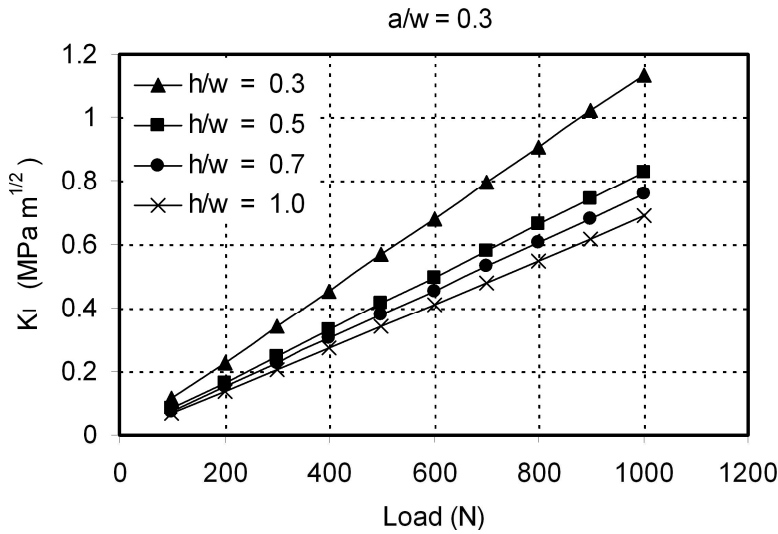


**Figure 9.** Variation of the measured  $K_I$  with applied load for  $a/w = 0.3$ .

this, the trend that the magnitude of the measured SIF is increasing with the increase in load is also in agreement with the theoretical predictions [Sanford 2003; Gdoutos 1990]. Further, the magnitude of SIF increases with decreasing  $h/w$ . Table 3 also provides normalized SIFs ( $F_I$ ), which are found to be independent of applied loads. Therefore a single value corresponding to a configuration is presented in the table.

Plots of the measured strain data as a function of the applied load for  $a/w = 0.5$  and  $h/w = 0.3$ , 0.5, 0.7, 1.0 were found to be very similar to the case of  $a/w = 0.3$ , and the corresponding averaged

Load (N)	$K_I$ (MPa $\sqrt{m}$ )			
	$a/w = 0.3$	$a/w = 0.5$	$a/w = 0.7$	$a/w = 1.0$
100	0.1132	0.0827	0.0757	0.0687
200	0.2265	0.1653	0.1513	0.1374
300	0.3397	0.2480	0.2270	0.2061
400	0.4529	0.3307	0.3027	0.2748
500	0.5662	0.4133	0.3783	0.3434
600	0.6794	0.4960	0.4540	0.4121
700	0.7926	0.5787	0.5297	0.4808
800	0.9059	0.6613	0.6053	0.5495
900	1.0191	0.7440	0.6810	0.6182
1000	1.1323	0.8267	0.7567	0.6869
$F_I$	2.7098	1.9783	1.8108	1.6438

**Table 3.** Measured  $K_I$  values at different loads for  $a/w = 0.3$ , and load-independent normalized SIFs (last row).

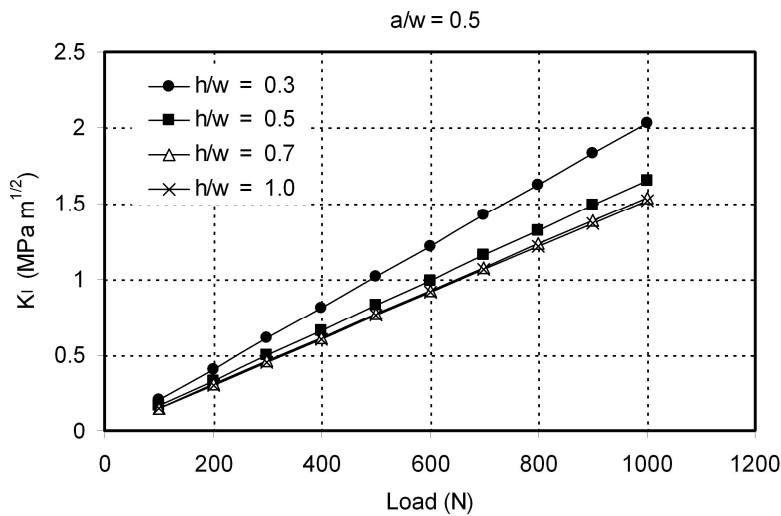


**Figure 10.** Variation of the measured  $K_I$  with applied load for  $a/w = 0.5$ .

measured SIFs at different applied loads are shown in Table 4. Figure 10 shows the graph of averaged measured SIFs as function of the applied load. As in the case of  $a/w = 0.3$ , the increase of the SIF with decreasing  $h/w$  and increasing values of the applied loads are in line with the theory. The normalized SIFs for  $h/w = 0.3, 0.5, 0.7$ , and  $1.0$  also appear in Table 4.

The measured  $F_I$  using strain gages and the computed normalized SIFs using FEA of semi-infinite and fully finite edge-cracked plate appear in Table 5. For comparison, the table also shows the analytical values of normalized SIFs [Tada et al. 2000] for semi-infinite plates ( $h/w = 1.0$ ). The discrepancy between

Load (N)	$K_I$ (MPa $\sqrt{m}$ )			
	$a/w = 0.3$	$a/w = 0.5$	$a/w = 0.7$	$a/w = 1.0$
100	0.2031	0.1654	0.1540	0.1520
200	0.4063	0.3308	0.3081	0.3040
300	0.6094	0.4962	0.4621	0.4560
400	0.8126	0.6616	0.6162	0.6080
500	1.0157	0.8270	0.7702	0.7600
600	1.2189	0.9923	0.9242	0.9120
700	1.4220	1.1577	1.0783	1.0639
800	1.6252	1.3231	1.2323	1.2159
900	1.8283	1.4885	1.3864	1.3679
1000	2.0315	1.6539	1.5404	1.5199
$F_I$	3.7666	3.0665	2.8561	2.8181

**Table 4.** Measured  $K_I$  values at different loads for  $a/w = 0.5$ , and load-independent normalized SIFs (last row).

$h/w$	$F_I$ ( $a/w = 0.3$ )			$F_I$ ( $a/w = 0.5$ )		
	numerical	experimental	analytic	numerical	experimental	analytic
0.3	2.5390	2.7098 (6.7%)	—	4.0308	3.7666 (6.6%)	—
0.5	1.8486	1.9783 (7.0%)	—	3.0060	3.0665 (2.0%)	—
0.7	1.6938	1.8108 (6.9%)	—	2.8514	2.8561 (0.2%)	—
1.0	1.6622	1.6438 (1.1%)	1.6624	2.8250	2.8181 (0.2%)	2.8291

**Table 5.** FE-computed, experimentally measured, and (where available) analytic values of  $F_I$  for edge-cracked plate and two choices of  $a/w$ . Bracketed values are absolute values of relative error. Analytic solutions are from [Tada et al. 2000].

the experimentally determined and FE-computed values, ranging from 0.2% to 7%, shows (assuming the FE-computed values to be exact) that the experimental method is substantially accurate in spite of the relatively large gage (3 mm active length). Excellent agreement is also observed between the measured and the theoretical normalized SIFs of semi-infinite plates.

Probable reasons for the somewhat larger errors (up to 7%) appearing in Table 5 are: (a) In all cases the cracks (fine slits) were made by pressing a razor blade through a distance of 2 mm; although great care was taken, it is difficult to control this length precisely. (b) When the razor blade is employed, the crack front at times is not precisely normal to the sheet surface. Similar observations were made in [Williams and Ewing 1972].

The measured and computed SIFs are shown in Figure 11, in order to assess the usefulness of the strain gage method of Dally and Sanford [1987] in combination with PMMA specimens for measuring the accurate SIFs. We see that either the results of Table 1 or the graphs in Figure 11 may be employed for SIFs of finite width and finite height edge-cracked plates subject to uniform tension.

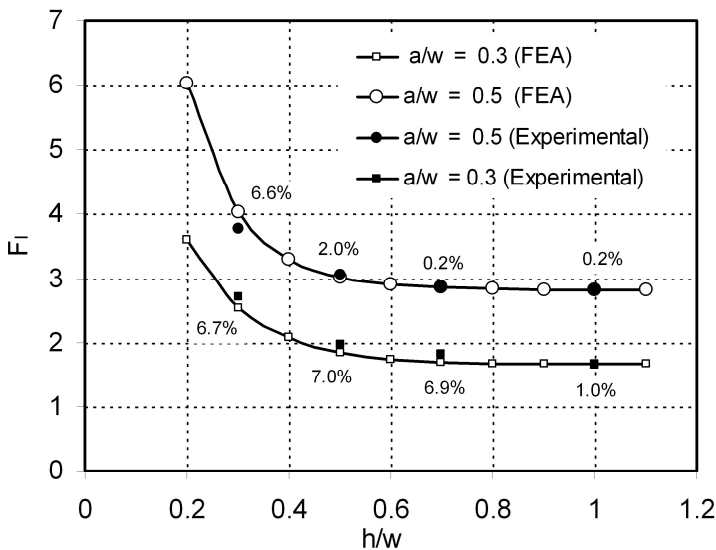


**Figure 11.** Comparison of measured and computed values of the normalized SIF.



## 7. Conclusions

The present investigation outlines various reasons which prevented the extensive application of the strain gage methods in determination of the accurate mode I SIFs. An experimental program is devised which includes the use of PMMA specimens so as to make the single strain gage method of [Dally and Sanford 1987] a more powerful and attractive experimental technique. The effectiveness of use of PMMA specimens in conjunction with the Dally and Sanford technique in measuring accurate opening mode stress intensity factors was demonstrated in the present investigation. Monotonically increasing load experiments were performed on the finite width and finite height PMMA edge-cracked specimens and strains were measured using 3 mm active length strain gages. Various trends of the experimental results are in excellent agreement with the LEFM theory. Moreover, a good agreement has also been observed between computed SIFs using FEA and the measured SIFs using the relatively large strain gages. The present investigation attempts to suggest accurate SIFs of the fully finite edge-cracked plates and subjected to uniform tension. The results of the present work clearly demonstrate that the single strain gage technique of Dally and Sanford can be used more effectively in combination with the PMMA specimens and can become a very useful tool for measurement of accurate opening mode SIFs of the complex configurations yet with relatively large gages.

## Acknowledgement

The authors are thankful to the staffs of the central workshop, strength of materials laboratory and Prof. H. B. Nemade of the Indian Institute of Technology, Guwahati for their constant help during the present work.

## References

- [Amir et al. 1989] A. D. K. Amir, N. S. Murthy, and N. G. Raju, "Stress intensity factor determination of radially cracked circular rings subjected to tension using photoelastic technique", *Engng. Fract. Mech.* **32** (1989), 403–408.
- [ANSYS 2005] "ANSYS POST1-crack analysis", in *Theory reference manual*, ANSYS, Inc., 2005.
- [Barsoum 1976] R. S. Barsoum, "On the use of isoparametric finite elements in linear fracture mechanics", *Int. J. Num. Meth. Engng.* **10** (1976), 25–37.
- [Berger and Dally 1988] J. R. Berger and J. W. Dally, "An overdeterministic approach for measuring using strain gages", *Exp. Mech.* **28** (1988), 142–145.
- [Biak et al. 1995] M. C. Biak, S. H. Choi, J. S. Hawong, and J. D. Kwon, "Determination of stress-intensity factors by the method of caustics in anisotropic materials", *Exp. Mech.* **35** (1995), 137–143.
- [Bonesteel et al. 1978] R. M. Bonesteel, D. E. Pipers, and A. T. Davinroy, "Compliance and calibration of double cantilever beam (DCB) specimens", *Engng. Fract. Mech.* **10** (1978), 425–428.
- [Broek 1982] D. Broek, *Elementary engineering fracture mechanics*, The Hague, 1982.
- [Chan and Chow 1979] W. Y. Chan and C. L. Chow, "Photoelastic stress intensity determination of circular-sector crack in rectangular plate", in *Proceedings of the Society for Experimental Stress Analysis Spring meeting* (San Francisco, 1979), 1979.
- [Dally and Berger 1986] J. W. Dally and J. R. Berger, "A strain gage method for determining and in a mixed mode stress field", in *Proceedings of the SEM spring conference on experimental mechanics* (New Orleans, LA, 1986), Society for Experimental Mechanics, Bethel, CT, 1986.
- [Dally and Berger 1993] J. W. Dally and J. R. Berger, "The role of the electrical resistance strain gauge in fracture research", pp. 1–39 in *Experimental techniques in fracture mechanics*, edited by J. S. Epstein, VCH, New York, 1993.

- [Dally and Riley 1991] J. W. Dally and W. F. Riley, "Experimental stress analysis", *McGraw-Hill* (1991).
- [Dally and Sanford 1987] J. W. Dally and R. J. Sanford, "Strain gage methods for measuring the opening mode stress intensity factor", *Exp. Mech.* **27** (1987), 381–388.
- [Freese and Tracey 1976] C. E. Freese and D. M. Tracey, "The natural isoparametric triangle versus collapsed quadrilateral for elastic crack analysis", *Int. J. Fract.* **12** (1976), R767–R770.
- [Gdoutos 1990] E. E. Gdoutos, *Fracture mechanics criteria and applications*, Dordrecht, 1990.
- [Gdoutos and Theocaris 1978] E. E. Gdoutos and P. S. Theocaris, "A photoelastic determination of mixed-mode stress intensity factors", *Exp. Mech.* **18** (1978), 87–96.
- [Hyde and Warrior 1990] T. H. Hyde and N. A. Warrior, "An improved method for determination of photoelastic stress intensity factors using the Westergaard stress function", *Int. J. Mech. Sci.* **32** (1990), 265–273.
- [Irwin 1957] G. R. Irwin, "Analysis of stresses and strains near the end of a crack traversing a plate", *J. Appl. Mech.* **24** (1957), 361–364.
- [Itoh et al. 1988] Y. Z. Itoh, T. Murakami, and H. Kashiwaya, "Proportional extrapolation techniques for determining stress intensity factors", *Engng. Fract. Mech.* **31** (1988), 297–308.
- [Jr 1981] J. C. N. Jr, "Stress-intensity factors and crack-opening displacements for round compact specimens", *Int. J. Fract.* **17** (1981), 567–578.
- [Katsamanis and Delides 1988] F. G. Katsamanis and C. G. Delides, "Fracture surface energy measurements of PMMA: A new experimental approach", *J. Phys. D Appl. Phys.* **21** (1988), 79–86.
- [Konsta-Gdoutos 1996] M. Konsta-Gdoutos, "Limitations in mixed-mode stress intensity factor evaluation by the method of caustics", *Engng. Fract. Mech.* **55** (1996), 371–382.
- [Kuang and Chen 1995] J. H. Kuang and L. S. Chen, "A single strain gage method for measurement", *Engng. Fract. Mech.* **51** (1995), 871–878.
- [Lee and Hong 1993] O. S. Lee and S. K. Hong, "Determination of stress intensity factors and J-integrals using the method of caustics", *Engng. Fract. Mech.* **44** (1993), 981–989.
- [Maccagno and Knott 1989] T. M. Maccagno and J. F. Knott, "The fracture behaviour of PMMA in mixed modes I and II", *Engng. Fract. Mech.* **34** (1989), 65–86.
- [Marloff et al. 1971] R. H. Marloff, M. M. Leven, T. N. Ringler, and R. L. Johnson, "Photoelastic determination of stress-intensity factors", *Exp. Mech.* **11** (1971), 529–539.
- [Mukherjee and Burns 1972] B. Mukherjee and D. J. Burns, "Growth of part-through thickness fatigue cracks in sheet Polymethylmethacrylate", *Engng. Fract. Mech.* **4** (1972), 675–685.
- [Murakami 1987] Y. Murakami (editor), *Stress intensity factors handbook*, vol. 1, Pergamon, Oxford, 1987.
- [Nurse et al. 1994] A. D. Nurse, E. W. O'Brien, and E. A. Patterson, "Stress intensity factors for cracks at fastener holes", *Fatigue Fract. Eng. Mater. Struct.* **17** (1994), 791–799.
- [Pang 1993] H. L. J. Pang, "Linear elastic fracture mechanics benchmarks: 2D finite element test cases", *Engng. Fract. Mech.* **44** (1993), 741–751.
- [Parnas and Bilir 1996] L. Parnas and O. G. Bilir, "Strain gage methods for measurement of opening mode stress intensity factor", *Engng. Fract. Mech.* **55** (1996), 485–492.
- [Sanford 1979] R. J. Sanford, "A critical re-examination of the Westergaard method for solving opening-mode crack problems", *Mech. Res. Comm.* **6** (1979), 289–294.
- [Sanford 2003] R. J. Sanford, *Principles of fracture mechanics*, Upper Saddle River, NJ, 2003.
- [Srikanth 2006] M. V. Srikanth, *Experimental determination of mode I and mixed mode stress intensity factors using strain gage technique*, Dissertation, Indian Institute of Technology Guwahati, 2006.
- [Swain 2007] P. K. Swain, *Comparison between various displacement based stress intensity factor computation techniques*, Dissertation, Indian Institute of Technology Guwahati, 2007.
- [Swamy 2007] S. Swamy, *Experimental determination of mode I stress intensity factors using strain gage technique*, Dissertation, Indian Institute of Technology Guwahati, 2007.

- [Tada et al. 2000] H. Tada, P. C. Paris, and G. R. Irwin (editors), *The stress analysis of cracks handbook*, ASME, New York, 2000.
- [Theocaris 1970] P. S. Theocaris, "Local yielding around a crack tip in Plexiglas", *J. Appl. Mech.* **37** (1970), 409–415.
- [Wei and Zhao 1997] J. Wei and J. H. Zhao, "A two-strain-gage technique for determining mode I stress-intensity factor", *Theor. Appl. Fract. Mech.* **28** (1997), 135–140.
- [Williams 1957] M. L. Williams, "On the stress distribution at the base of a stationary crack", *J. Appl. Mech.* **24** (1957), 109–114.
- [Williams and Ewing 1972] J. G. Williams and P. D. Ewing, "Fracture under complex stress: the angle crack problem", *Int. J. Fract.* **8** (1972), 441–446.
- [Xu et al. 2004] W. Xu, X. F. Yao, M. Q. Xu, G. C. Jin, and Y. H. Yeh, "Fracture characterizations of V-notch tip in PMMA polymer material", *Poly. Test.* **23** (2004), 509–515.

Received 4 Dec 2007. Revised 22 Apr 2008. Accepted 18 Jul 2008.

S. SWAMY: [s.swamy@iitg.ernet.in](mailto:s.swamy@iitg.ernet.in)  
*Mahindra and Mahindra Limited, Pune, India*

M. V. SRIKANTH: [venkatasrikanth.manda@wipro.com](mailto:venkatasrikanth.manda@wipro.com)  
*Wipro Technologies, Cyber City, Hyderabad, India*

K. S. R. K. MURTHY: [ksrkm@iitg.ernet.in](mailto:ksrkm@iitg.ernet.in)  
*Department of Mechanical Engineering, Indian Institute of Technology, Guwahati 781 039, Assam, India*

P. S. ROBI: [psr@iitg.ernet.in](mailto:psr@iitg.ernet.in)  
*Department of Mechanical Engineering, Indian Institute of Technology, Guwahati 781 039, Assam, India*

